Korean J. Chem. Eng., **18**(1), 14-20 (2001)

Spatial Structures Evolving from Homogeneous Media in Immobilized Enzyme Systems

Sang Hwan Kim†, Jun-Bong Kim and Hyung-Sang Park*

Department of Chemical Engineering, Konkuk University, Seoul 143-701, Korea
*Department of Chemical Engineering, Sogang University, Seoul 121-742, Korea
(*Received 6 September 1999 • accepted 20 December 2000*)

Abstract−The detailed pattern of spatial structures for the reaction-diffusion system involving substrate-inhibited reactions on immobilized uricase enzyme was studied. Depending on the governing parameters, three basic solutions may exist and there are two kinds of possible branching, either successive primary bifurcation from a basic trivial branch or consecutive secondary bifurcation. In both cases the branching follows the sequence of symmetric → asymmetric → symmetric, and so forth. The emergence of subsequently more complex spatial structures with the increasing length of systems suggests a close similarity to gradual buildup of complex morphogenetic patterns in developmental biology.

Key words: Spatial Structures, Thomas Model, Immobilized Enzyme Systems, Bifurcation, Multiple Steady States

INTRODUCTION

A number of nonlinear reaction-diffusion systems can possess more than one stable steady-state solution. Some of these solutions can be spatially uniform while the others can feature non-uniform distribution in space (so called spatial structures). Existence of spatially periodic solutions, conditions necessary for their occurrence, and multiplicity are questions of considerable interest.

The emergence of spatial structures from a perfectly homogeneous medium is analogous to pattern formation in developmental biology [Turing, 1952; Goodwin, 1969; Goldbeter, 1973; Murray, 1982; Gierer, 1981; Catalano, 1981], Benard convection in hydrodynamics [Chandrasekhar, 1981], and the non-uniform distribution of concentration and/or temperature in chemical reaction-diffusion systems [Schmitz and Tsotsis, 1971, 1983; Erk and Dudukovic, 1983]. The dissipative structure for the "Brusselator", a simple autocatalytic trimolecular reaction scheme, has been extensively studied by Prigogine and his associates [Glansdorff and Prigogine, 1971; Prigogine and Lefever, 1968; Herschkowitz-Kaufman and Nicolis, 1972; Erneux and Herschkowitz-Kaufman, 1979; Herschkowitz-Kaufman, 1975], Kubicek et al. [1978], and Janssen et al. [1983]. They have reported many interesting phenomena such as multiple symmetric and asymmetric steady states, homogeneous periodic solutions, and travelling, standing or rotating waves.

In this paper, we analyzed the properties of the diffusion-reaction system with the substrate-inhibited immobilized enzyme kinetics, frequently in the literature referred to as the "Thomas model" [Kernevez et al., 1982]. The Thomas model has been proposed as one of the possible mechanisms for pattern formation in developmental biology. Emphasis is placed on the pattern of spatial structures emerging from the homogeneous medium in an immobilized enzyme reaction-diffusion system. We will show that qualitative features observed for an auto-catalytic reaction system remain unchanged.

GOVERNING EQUATIONS

The Thomas model for the substrate-inhibited kinetics on immobilized uricase enzyme [Kernevez et al., 1982] involves the following arrangement. Essentially, two chemicals, uric acid (S) and oxygen (A), diffuse from a reservoir maintained at constant concentrations S_0 and A_0 through an inactive membrane of thickness L_1 onto a membrane of thickness L_2 (≃50 μm) containing the immobilized enzyme uricase as shown in Fig. 1. The two-dimensional plate is closed on the ends and immersed in the reservoir. The uric acid and oxygen diffuse on this membrane with diffusion coefficients D_S and D_A and react under the catalytic action of uricase enzymes subject to the following reaction rate expression:

$$R = V_m A\, S/(K_m + S + S^2/K_S) \tag{1}$$

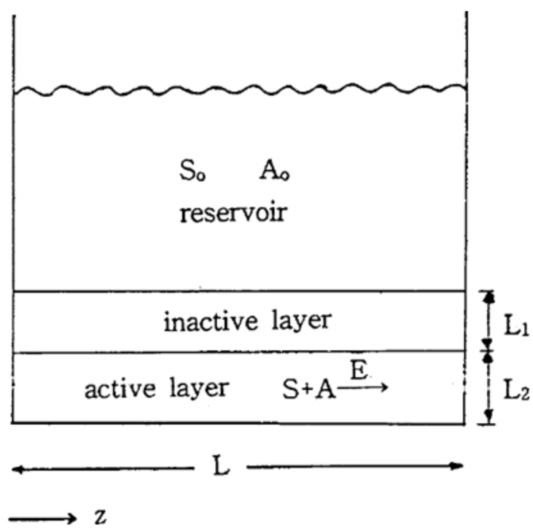

Fig. 1. One-dimensional immobilized uricase system.

†To whom correspondence should be addressed.
E-mail: sanghkim@konkuk.ac.kr

Here V_m, K_m, and K_s are constants. This reaction scheme exhibits the characteristics of the substrate-inhibited reaction where K_s is related to the substrate inhibition rate. The small values of K_s imply the large inhibition of substrates. For fixed concentrations of A, the reaction rate of substrate-inhibited kinetics may be similar to that of Michaelis-Menten kinetics for the low concentrations of S.

Mass balances yield the following differential equations:

$$\frac{\partial S}{\partial t}=D_S\frac{\partial^2 S}{\partial z^2}+P_S(S_O-S)-\frac{V_m AS}{K_m+S+S^2/K_S} \tag{2}$$

$$\frac{\partial A}{\partial t}=D_A\frac{\partial^2 A}{\partial z^2}+P_A(A_O-A)-\frac{V_m AS}{K_m+S+S^2/K_S}. \tag{3}$$

For simplicity we assume that (i) there exists a concentration gradient only in the z-direction and (ii) homogeneous distribution of the enzyme uricase on the active layer.

A set of differential equations, Eqs. (2) and (3), can be rewritten in the following dimensionless form:

$$\frac{\partial s}{\partial \tau}=\frac{\partial^2 s}{\partial x^2}+\gamma\left\{(s_O-s)-\frac{\rho as}{1+s+ks^2}\right\}=\frac{\partial^2 s}{\partial x^2}+f(s,\ a) \tag{4}$$

$$\frac{\partial a}{\partial \tau}=\beta\frac{\partial^2 s}{\partial x^2}+\gamma\left\{\alpha(a_O-a)-\frac{\rho as}{1+s+ks^2}\right\}=\beta\frac{\partial^2 a}{\partial x^2}+g(s,\ a) \tag{5}$$

subject to Neumann boundary conditions

$$x=0;\quad \frac{\partial s}{\partial x}=\frac{\partial a}{\partial x}=0 \tag{6}$$

$$x=1;\quad \frac{\partial s}{\partial x}=\frac{\partial a}{\partial x}=0. \tag{7}$$

Here we have denoted s and a the dimensionless concentrations of uric acid (S) and oxygen (A), respectively, α the ratio of mass transfer coefficients of oxygen to uric acid in the inactive layer, β the ratio of diffusion coefficients of oxygen to uric acid in the active layer, x the dimensionless length, k the dimensionless inhibition rate and τ the dimensionless time. The various quantities in Eqs. (4) and (5) are defined as follows:

$$\begin{aligned}
&s=\frac{S}{K_m}\quad a=\frac{A}{K_m}\quad x=\frac{z}{L}\quad \tau=\frac{D_S}{L^2}t\\
&\alpha=\frac{P_A}{P_S}\quad \beta=\frac{D_A}{D_S}\quad \gamma=\frac{P_S L^2}{D_S}\\
&\rho=\frac{V_m}{P_S}\quad k=\frac{V_m}{K_S}.
\end{aligned} \tag{8}$$

A uniform steady state $(\tilde{s},\ \tilde{a})$ is obtained by solving the following algebraic equations simultaneously:

$$f(\tilde{s},\ \tilde{a})=s_O-\tilde{s}-\frac{\rho\tilde{a}\tilde{s}}{1+\tilde{s}+k\tilde{s}^2}=0 \tag{9}$$

$$g(\tilde{s},\ \tilde{a})=\alpha(a_O-\tilde{a})-\frac{\rho\tilde{a}\tilde{s}}{1+\tilde{s}+k\tilde{s}^2}=0. \tag{10}$$

The uniform states, which are also called basic solutions, are described by Eq. (11)

$$\tilde{s}^3+p\tilde{s}^2+q\tilde{s}+r=0 \text{ and } \tilde{a}=a_O+\frac{1}{\alpha}(\tilde{s}-s_O) \tag{11}$$

where

$$p=\frac{1}{k}\left(1-ks_O+\frac{\rho}{\alpha}\right) \tag{12}$$

$$q=\frac{1}{k}\left(1+\rho a_O-s_O-\frac{\rho s_O}{\alpha}\right) \tag{13}$$

$$r=-\frac{s_O}{k}. \tag{14}$$

The number of basic solutions (one, two or three) depends on the values of governing parameters, k, s_O, a_O, α and ρ and shows no relationship with the parameters, γ and β. It is noted that the number of basic solutions is independent on the ratio of diffusion coefficients of oxygen to uric acid in the active layer. In order to determine the number of basic solutions, Cardan's method [Hildebrand, 1968] for a cubic equation with real coefficients can be applied to Eq. (11). The parameter D in Eq. (15) determines the number of solutions in the following way:

$$D=\left(\frac{u}{3}\right)^3+\left(\frac{v}{2}\right)^2 \tag{15}$$

where

$$u=\frac{1}{k}\left(1+\rho a_O-s_O-\frac{\rho s_O}{\alpha}\right)-\frac{1}{3k^2}\left(1-ks_O+\frac{\rho}{\alpha}\right)^2 \tag{16}$$

$$\begin{aligned}
v=&-\frac{s_O}{k}-\frac{1}{3k^2}\left(1-ks_O+\frac{\rho}{\alpha}\right)\left(1+\rho a_O-s_O-\frac{\rho s_O}{\alpha}\right)\\
&+\frac{2}{27k^3}\left(1+\rho a_O-s_O-\frac{\rho s_O}{\alpha}\right)^3.
\end{aligned} \tag{17}$$

There can exist three, two or one basic solution for D<0, D=0 or D>0, respectively. The stability of basic solutions can be determined by the eigenvalues of the linearized operator $\mathcal{L}$,

$$\mathcal{L}=\begin{vmatrix} \frac{d^2}{dx^2}+C_{11} & C_{12} \\ C_{21} & \beta\frac{d^2}{dx^2}+C_{22} \end{vmatrix}, \tag{18}$$

where

$$C=\begin{vmatrix} C_{11} & C_{12} \\ C_{21} & C_{22} \end{vmatrix}=\begin{vmatrix} \frac{\partial f(\tilde{s},\ \tilde{a})}{\partial s} & \frac{\partial f(\tilde{s},\ \tilde{a})}{\partial a} \\ \frac{\partial g(\tilde{s},\ \tilde{a})}{\partial s} & \frac{\partial g(\tilde{s},\ \tilde{a})}{\partial a} \end{vmatrix}. \tag{19}$$

The basic solutions $(\tilde{s},\ \tilde{a})$ are stable if all eigenvalues of the operator $\mathcal{L}$ have negative real parts and unstable if there is at least one eigenvalue with positive real part.

For zero flux boundary conditions the eigenfunctions of the Laplacian operator in one-dimensional space can be expressed as cos $n\pi x$ (n=0, 1, 2, $\cdots$). Therefore, the stability of basic solutions is determined by the sign of the eigenvalues (ω_n) satisfying the following characteristic equation:

$$\omega_n^2-T_r\omega_n+\Delta=0 \tag{20}$$

where

$$T_r = -(n\pi)^2(1+\beta) + \gamma\left\{\frac{(k\tilde{s}^2-1)(s_o-\tilde{s})-\rho\tilde{s}^2}{1+\tilde{s}+k\tilde{s}^2} - 1 - \alpha\right\} \tag{21}$$

$$\Delta = p'\gamma^2 + q'\gamma + r'. \tag{22}$$

Here p', q' and r' are defined by

$$p' = \left\{1 - \frac{(k\tilde{s}^2-1)(s_o-\tilde{s})}{(1+\tilde{s}+k\tilde{s}^2)\tilde{s}}\right\}\left\{\alpha + \frac{\rho\tilde{s}}{1+\tilde{s}+k\tilde{s}^2}\right\} + \frac{\rho(k\tilde{s}^2-1)(s_o-\tilde{s})}{(1+\tilde{s}+k\tilde{s}^2)^2} \tag{23}$$

$$q' = (n\pi)^2\left\{\alpha+\beta+\frac{\rho\tilde{s}^2-\beta(k\tilde{s}^2-1)(s_o-\tilde{s})}{(1+\tilde{s}+k\tilde{s}^2)\tilde{s}}\right\} \tag{24}$$

$$r' = \beta(n\pi)^4. \tag{25}$$

Uniform steady states can be destabilized into two ways; through real eigenvalues (Re $\omega_n>0$, $I_m\ \omega_n=0$) or through complex ones (Re $\omega_n>0$, $I_m\ \omega_n\neq 0$). In the former case the instability of uniform steady states is ascertained when Δ is greater than zero ($\Delta>0$). Therefore, non-uniform steady states can occur at the critical values of the bifurcation parameter γ satisfying Eq. (22) when Δ is set to zero. These values for γ are called the primary bifurcation points (γ^*) on the basic branches. The successive primary bifurcation points can be easily calculated for a set of discrete values of the wave number n.

Even though we can locate the primary bifurcation points analytically, it is very difficult to calculate the whole parametric dependence of solutions and secondary bifurcation points in an analytical way. Therefore, we will resort to a numerical scheme for calculating the bifurcation diagram.

NUMERICAL RESULTS

In order to investigate the parametric dependence of solution branches for a set of parabolic partial differential equations, Eqs. (4)-(7), we approximate the differential operator in space by the Stormer-Numerov finite difference scheme [Kim, 1989; Doedel, 1980] featuring the $0(h^4)$ accuracy where h is denoted by step size in space. The complete bifurcation analysis of a resulting system of ordinary differential equations was peformed by using the software package AUTO [Kim, 1988]. The detailed algorithm for discretization of the differential operator with the $0(h^4)$ accuracy will be found elsewhere [Doedel, 1980]. There are seven parameters, α, β, γ, ρ, k, s_o, and a_o in Eqs. (4) and (5). Among them the variable γ, representing the dimensionless length of the system, is most important. Therefore, we selected the variable γ as the bifurcation parameter in this study.

The values of governing parameters are shown in Table 1. Ten grid points in space were used to discretize the differential operator for the bifurcation analysis. The numerical calculation was performed on CDC 730 and the error of integration was controlled to six significant decimal places.

Table 1. Parametric values in substrate-inhibited enzyme systems

s_O=102.5
a_O=79.2
α=1.45
β=5.0
k=0.1
ρ=13.0

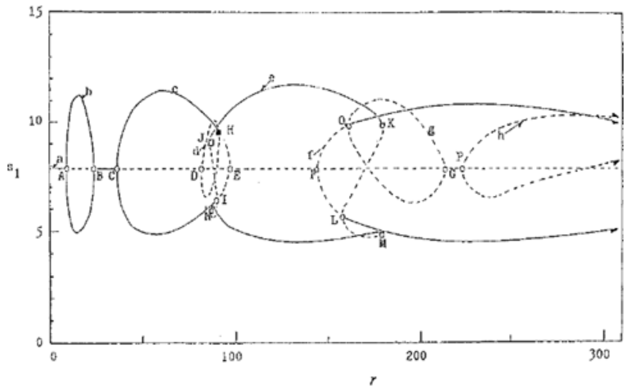

Fig. 2. Bifurcation diagram for 10-point discretization of immobilized uricase plate.
—— stable steady state, ---- unstable steady state, ○ bifurcation point, □ limit point, ■ bifurcation and limit point.

The complete bifurcation diagram "s_i versus γ" is displayed in Fig. 2. The subscript i in s_i on the ordinate represents the grid point in space. In this figure the solid and dotted lines portray the stable and unstable steady-state solutions, respectively. The small letters (**a**, **b**, ···, **h**) stand for the branches of steady state solutions while the capital letters (A, B, ···, P) represent the bifurcation and limit points. Open circles and squares denote the bifurcation and limit points, respectively. The bifurcation-limit points are also represented by the closed squares in this figure. The bifurcation and limit points detected in the system considered are summarized in Table 2.

For all values of γ there exists one basic trivial branch, $\tilde{s}$ =

Table 2. Summary of bifurcation and limit points

Point	γ	s_1	Type*
A	9.1	7.84	BP
B	23.9	7.84	BP
C	36.3	7.84	BP
D	81.2	7.84	BP
E	95.45	7.84	BP
F	143.5	7.84	BP
G	223.4	7.84	BP
H	90.2	9.54	BP+LP
I	89.2	6.32	BP
J	85.6	9.01	LP
K	180.3	9.83	LP
L	158.7	5.67	BP
M	180.3	4.93	LP
N	85.6	6.02	LP
O	161.1	9.88	BP
P	213.5	7.84	BP

*BP: Bifurcation point
LP: Limit point
BP+LP: Bifurcation-limit point

7.8479, $\tilde{a}$=13.9227 which is in good agreement with the analytical results obtained from Eq. (11). The positive value of D (D≅2.4674×10^5) in Eq. (15) verifies the existence of a unique basic branch. The primary bifurcation points are in full agreement with those obtained from Eq. (22) analytically. The branch '**a**' of symmetric profiles corresponds to the branch of uniform steady states or a basic branch. There are several primary bifurcation points (A, B, C, D, E, F, G, P) on the basic branch '**a**'. The bifurcation points A and B, occurring at the branch '**a**' of symmetric solutions, give rise to a closed branch '**b**' of asymmetric solutions. At the bifurcation points C and E, on the basic branch '**a**', a closed branch '**c**' of symmetric solutions emerges. From the point D on the basic branch '**a**', a closed loop of asymmetric solutions, branch '**d**' results. A typical bifurcation-limit point H is displayed in Fig. 2. This point is a bifurcation point of the branch '**c**' of symmetric solutions because an asymmetrical solution may emerge. On the other hand, H is a limit point at the branch '**d**' of the asymmetric solutions. At this point two asymmetric solutions collapse into a symmetric one.

It may be inferred from the result obtained on the branch '**a**' to '**d**' that a homogeneous steady state exists for the small size of system (γ<9.1) and this stable steady state does not change to any perturbation in the concentration of uric acid and oxygen. As the length of immobilized enzyme systems is increased (9.1<γ<23.9), the homogeneous steady state may be driven unstable by diffusion and asymmetric heterogeneous patterns are obtained. These spatial patterns are relatively simple, asymmetric, and stable as shown in Fig. 5. The pattern is composed of two regions of substrate concentrations S. One is higher concentration region of S(s>$\tilde{s}$) and the other is lower concentration region of S(s<$\tilde{s}$). As the values of γ increase, the steep profiles of substrate concentrations S are developed. These have been studied by Kernevez [1982] and Murray [1982]. The former applied the diffusion-driven instability to sequential compartment formation in drosophila wings using Kauffamn's model and the latter proposed the mechanism for generating the prepattern for animal coat markings. With further increasing size of systems (23.9<γ<36.3) the basic branch '**a**' becomes again stable resulting from exchange of stabilities between points B and C. There also exists the stable homogeneous steady state. This observation may indicate the predominance of reaction kinetics in a certain size of system (23.9<γ<36.3). The homogeneous steady state becomes unstable and heterogeneous patterns are obtained for larger size of systems (γ>36.3).

At the branch '**c**' of symmetric solutions there is a bifurcation point (secondary bifurcation point) I which gives rise to a branch '**e**' of asymmetric solutions, see Fig. 3. At point I the bifurcation is backward with an exchange of stabilities and the secondary bifur-

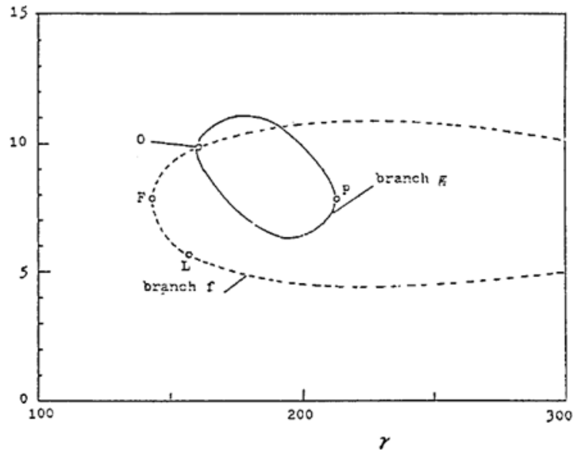

Fig. 4. Bifurcation diagram, branch f (asymmetric solutions).

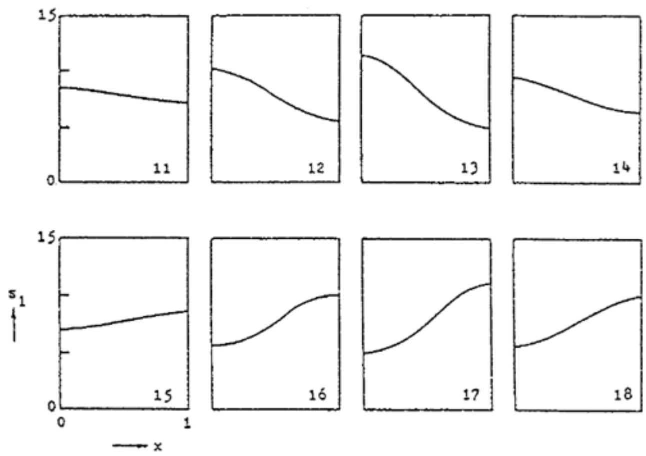

Fig. 5. Spatial profiles at particular points on branch b.

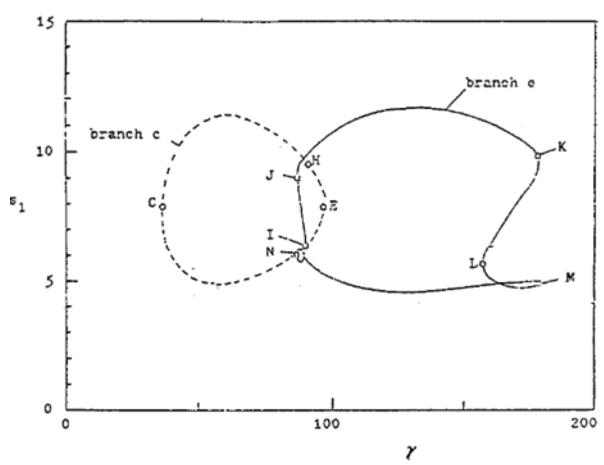

Fig. 3. Bifurcation diagram, branch e (asymmetric solutions).

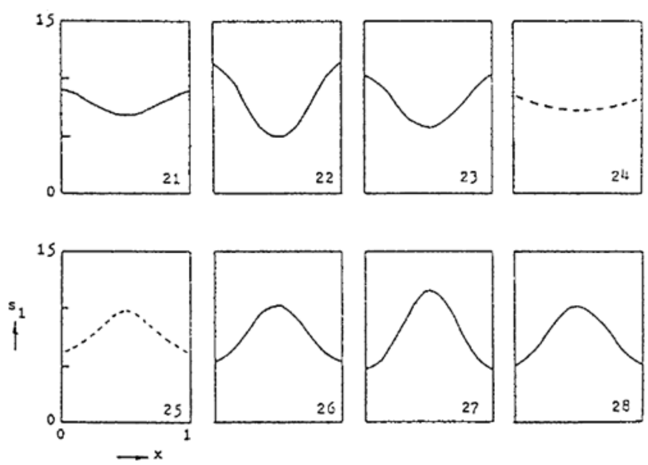

Fig. 6. Spatial profiles at particular points on branch c.

cation branch is unstable at that point. Four limit points (J, K, M and N) occurring at the above-mentioned branch '**e**' are depicted. From the point F on the basic branch '**a**', a branch '**f**' of symmetric solutions emerges, see Fig. 2. At the bifurcation point 0, a branch of asymmetric solution '**g**' results as depicted in Fig. 4. In Figs. 3 and 4 the solid and dotted lines represent the asymmetric and symmetric solutions, respectively. Another branch '**h**' of asymmetric solutions is created from the bifurcation point P on the basic branch '**a**', see Fig. 2.

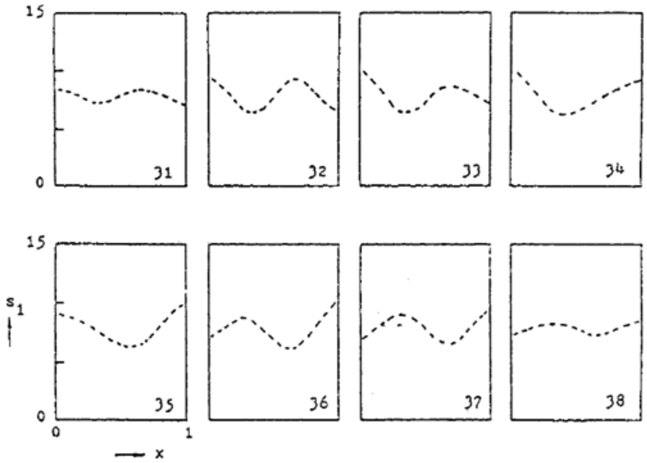

Fig. 7. Spatial profiles at particular points on branch d.

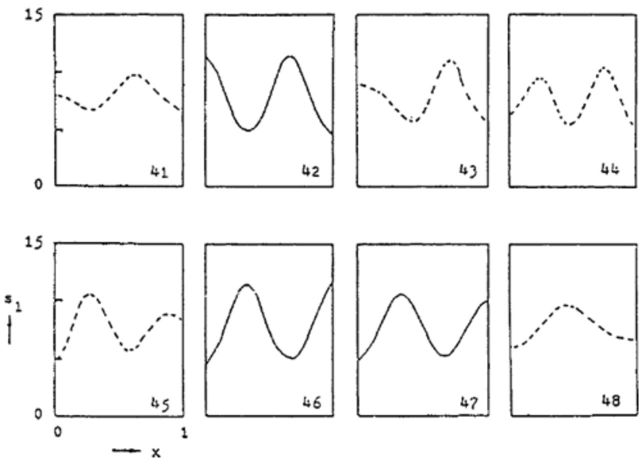

Fig. 8. Spatial profiles at particular points on branch e.

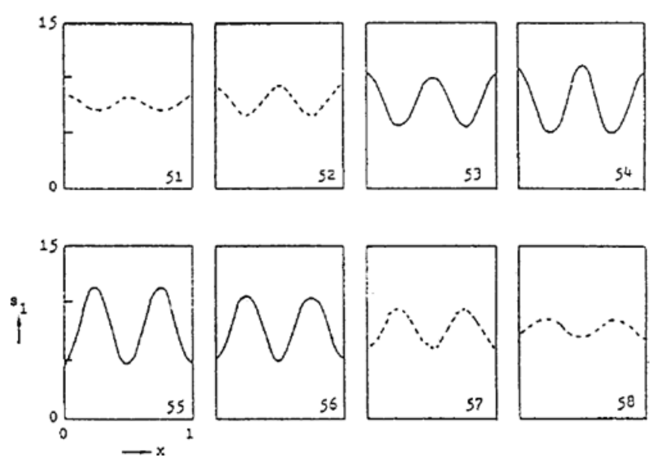

Fig. 9. Spatial profiles at particular points on branch f.

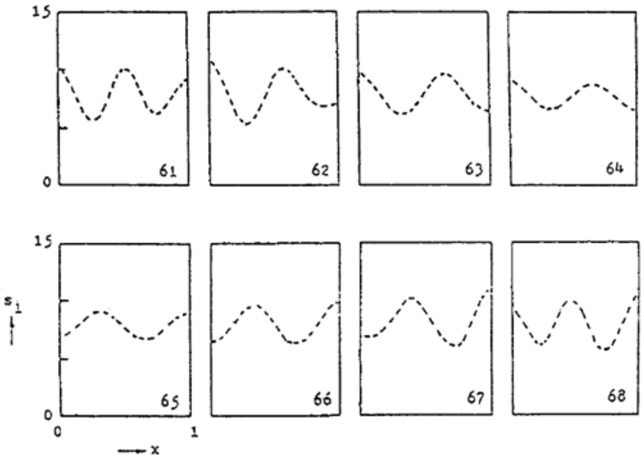

Fig. 10. Spatial profiles at particular points on branch g.

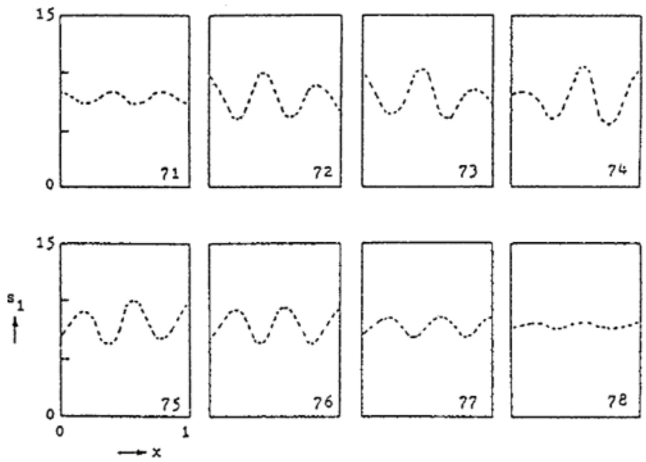

Fig. 11. Spatial profiles at particular points on branch h.

The spatial profiles at particular points on the branches in Fig. 2, are depicted in Figs. 5-11. In these figures the solid lines denote the stable steady states while the dotted lines represent the unstable steady solutions. The γ values of numbered points are summarized in Table 3. The basic branch '**a**' becomes always unstable for larger values of γ (γ>36.3). For smaller values of γ as shown in Figs. 5 and 6, the spatial patterns are relatively simple because there exist one region of higher substrate concentration ($s>\tilde{s}$) and one region of lower substrate concentration ($s<\tilde{s}$). As the values of γ increase further, the spatial patterns become complex with two regions of higher substrate concentration and two regions of lower substrate concentration alternately as shown in Figs. 7 and 8. For the higher values of γ the spatial patterns become more and more complex because three regions of higher and lower substrate concentration exist alternately as depicted in Figs. 9 and 11. Thus, the buildup of more complex patterns in compartment formation of drosophila wings, prepattern for animal coat markings and so forth, can be in part explained with these results. It is obvious that the length of the system (γ) predicts the emergence of more and more complex spatial structures. The branches of asymmetric solutions possess one typi-

Table 3. The γ values of important points

Branch	Point	γ	Branch	Point	γ
b	11	9.2(u)*	f	51	145.0(u)
	12	10.1(u)		52	150.2(u)
	13	16.8(u)		53	172.2(u)
	14	22.8(u)		54	223.4(u)
	15	23.7(l)		55	227.2(l)
	16	20.9(l)		56	172.5(l)
	17	17.3(l)		57	150.9(l)
	18	10.1(l)		58	145.1(l)
c	21	37.0(u)	g	61	162.5(u)
	22	65.0(u)		62	177.1(u)
	23	84.1(u)		63	199.6(u)
	24	95.0(u)		64	208.7(u)
	25	89.4(l)		65	208.7(l)
	26	79.2(l)		66	199.6(l)
	27	57.3(l)		67	182.6(l)
	28	45.2(l)		68	163.0(l)
d	31	81.7(u)	h	71	224.9(u)
	32	84.7(u)		72	249.4(u)
	33	86.1(u)		73	276.5(u)
	34	89.9(u)		74	295.3(l)
	35	89.9(l)		75	249.4(l)
	36	86.3(l)		76	236.9(l)
	37	83.9(l)		77	227.0(l)
	38	81.7(l)		78	223.4(l)
e	41	86.8(u)			
	42	134.8(u)			
	43	177.9(u)			
	44	160.1(l)			
	45	174.7(l)			
	46	129.7(l)			
	47	98.8(l)			
	48	89.1(l)			

*: u denotes the upper part of each branch from the basic '**a**' while l represents the lower part of it.

cal property, namely mirror image profiles. For instance, the asymmetric profiles on the identical branch (12 & 18, 31 & 38, 34 & 35 and 64 & 65) clearly show the characteristics of mirror images. One of the interesting things to note is the number of steady states. The multiplicity of steady states in Fig. 2 is summarized in Table 4.

CONCLUSIONS

The continuous dependence of the character and number of solutions on the bifurcation parameter γ for the Thomas model has shown that the primary bifurcation branches form the closed curves and three basic solutions at most are possible. The multiplicity of steady state solutions is expected and among them a countable number of solutions are stable.

There are two possible ways of branching the solutions. One is the successive branching from the primary bifurcation points on the basic branch. The other is consecutive branching, i.e., primary →secondary→tertiary→···. In both cases the branching is of the type symmetric→asymmetric→symmetric→···. The emergence of more and more complex spatial structures with increasing values of system size (γ) is similar to the gradual buildup of complex morphogenetic patterns in the developmental biology and deserves further study.

Table 4. Multiple steady states in immobilized enzyme systems

γ	Number of solutions (no. of stable solutions)
(0.0, 9.1)	1 (1)
(9.1, 23.9)	3 (2)
(23.9, 36.3)	1 (1)
(36.3, 81.2)	3 (2)
(81.2, 85.6)	5 (2)
(85.6, 89.2)	9 (4)
(89.2, 90.2)	7 (4)
(90.2, 95.4)	5 (2)
(95.4, 143.5)	3 (2)
(143.5, 158.7)	5 (2)
(158.7, 161.1)	7 (4)
(161.1, 180.3)	9 (4)
(180.3, 213.5)	5 (2)
(213.5, 223.4)	3 (2)
(223.4, 300.0)	5 (2)

ACKNOWLEDGEMENT

The bifurcation diagrams reported in this paper have been calculated by the bifurcation package AUTO which was provided by Dr. E. Doedel. Computer Science Department, Concordia Universety, Montreal, Canada. His assistance and discussion is sincerely appreciated.

NOMENCLATURE

A : concentration of oxygen
a : dimensionless concentration of oxygen $(=\frac{A}{K_m})$
C : Jacobian matrix defined by Eq. (20)
D : discriminant defined by Eq. (16)
D_S, D_A : diffusion coefficients of uric acid and oxygen in the active layer, respectively
f, g : reaction kinetic term defined by Eqs. (5) and (6)
k : dimensionless inhibition rate $(=\frac{V_m}{K_s})$
K_m, K_s : constants
L_1, L_2 : thickness of the inactive and active membrane layer, respectively
p', q', r' : constants defined by Eqs. (21) and (23)
P_S, P_A : mass transfer coefficients of uric acid and oxygen through inactive membrane, respectively
R : reaction rate defined by Eq. (1)
S : concentration of uric acid
s : dimensionless concentration of uric acid $(=\frac{S}{K_m})$

u : constant defined by Eq. (17)
v : constant defined by Eq. (18)
V_m : reaction rate constant
x : dimensionless length $(=\frac{z}{L})$
z : space coordinate

Greek Letters

α : ratio of mass transfer coefficients of oxygen to uric acid $(=\frac{P_A}{P_S})$
β : ratio of diffusion coefficients of oxygen to uric acid $(=\frac{D_A}{D_S})$
γ : dimensionless length $(=\frac{P_S L^2}{D_S})$
Δ : determinant defined by Eq. (23)
ρ : dimensionless reaction rate constant $(=\frac{V_m}{P_S})$
τ : dimensionless time $(=\frac{D_S}{L^2}t)$
ω : eigenvalues in Eq. (21)

Superscript

~ : steady state

Subscripts

i : grid point in space
n : wave number
o : condition at the surrounding reservoir

REFERENCES

Catalano, G., "A Mathematical Model for Pattern Formation in Biological Systems," *Physica*, **3D**, 439 (1981).

Chandrasekhar, S., "Hydrodynamics and Hydromagnetic Stability," Dover Publications, New York (1981).

Doedel, E., "Auto: A Program for Automatic Bifuriciation Analysis of Autonomous Systems," Proc. 10th Manitoba Conference on Numerical Mathematics and Computing, Winnipeg, Canada (1980).

Erk, H. F. and Dudukovic, M. P., "Self-Inhibited Rate in Gas-Solid Noncatalytic Reactions: The Rotten Apple Phenomena and Multipic Reaction Pathways," *IEC Fund.*, **22**, 55 (1983).

Erneux, T. and Herschkowitz-Kaufinan, M., "Bifurcation Diagram of a Model Chemical Reaction-1. Stability Changes of Time-Periodic Solutions," *Bull. of Math. Biol.*, **41**, 21 (1979).

Gierer, A., "Some Physical, Mathematical and Evolutionary Aspects of Biological Pattern Formation," *Phil. Trans. Roy. Soc.*, **B295**, 429 (1981).

Glansdorff, P. and Prigogine, T., "Thermodynamics of Structures, Stability and Fluctuations," Interscience, New York (1971).

Goldbeter, A., "Patterns of Spatiotemporal Organization in an Allosteric Enzyme Model," *Proc. Natl. Acad. Sci.*, **70**, 3255 (1973).

Goodwin, B. C., "A Phase-Shift Model for the Spatial and Temporal Organization of Developing Systems," *J. Theor. Biol.*, **25**, 49 (1969).

Herschkowitz-Kaufman, M. and Nicolis, G., "Localized Spatial Structures and Nonlinear Chemical Waves in Dissipative Systems," *J. of Chem. Phys.*, **56**, 1890 (1972).

Herschkowitz-Kaufman, M., "Bifurcation Analysis of Nonlinear Reaction-Diffusion Equations," *Bull. of Math. Biol.*, **37**, 589 (1975).

Hildebrand, F. B., "Finite-Difference Equations and Simulations," Prentice Hall, Englewood Cliffs, New Jersey (1968).

Janssen, R., Hlavacek, V. and Rompay, P., "Bifurcation Pattern in Reaction-Diffusion Dissipative Systems," *Z. Naturforch*, **38**, 487 (1983).

Kernevez, J. P., Joly, G., Duban, M. C., Bunow, B. and Thomas, D., "Hysteresis, Oscillations, and Pattern Formation in Realistic Immobilized Enzyme Systems," *J. Theor. Biol.*, **7**, 143 (1982).

Kim, S. H., "Application of Nonlinear Dynamic Analysis to Chemically Reacting Systems," Ph.D. Dissertation, State University of New York at Buffalo, Buffalo (1988).

Kim, S. H., "Stormer-Numerov Approximation for Numerical Solutions of Ordinary and Partial Differential Equations," *Korean J. Chem. Eng.*, **6**, 165 (1989).

Kubicek, M., Ryzler, V. and Marek, M., "Spatial Structures in a Reaction-Diffusion System-Detailed Analysis of the Brusselator," *Biophys. Chem.*, **8**, 235 (1978).

Murray, J. D., "Parameter Space for Turing Instability in Reaction-Diffusion Mechanism," *J. Theor. Biol.*, **98**, 143 (1982).

Prigogine, I. and Lefever, R., "Symmetry Breaking Instabilities in Dissipative Systems," *J. Chem. Phys.*, **48**, 1695 (1968).

Schmitz, R. A. and Tsotsis, T. T., "On the Possibility of Spatially Patterned States in Systems of Interacting Catalyst Particles," 72nd Annual Meeting of AIChE, San Francisco, U.S.A (1971).

Schmitz, R. A. and Tsotsis, T. T., "Spatially Patterned States in Systems of Interacting Catalyst Particles," *Chem. Eng. Sci.*, **38**, 1431 (1983).

Turing, A. M., "The Chemical Basis of Morphogenesis," *Phill. Trans. Roy. Soc.*, **B237**, 37 (1952).